A Cluster-Based Transmit Diversity Scheme for Asynchronous Joint Transmissions in Private Networks

Kim, Kyeong Jin; Guo, Jianlin; Orlik, Philip V.; Nagai, Yukimasa; Poor, H. Vincent

TR2021-075 June 12, 2021

Abstract

In this paper, a multiple cluster-based transmission diversity scheme is proposed for asynchronous joint transmissions (JT) in private networks, in which the use of multiple clusters or small cells is preferable to increase transmission speeds, reduce latency, and bring transmissions closer to the users. To increase the spectral efficiency and coverage, and to achieve flexible spatial degrees of freedom, a distributed remote radio unit system (dRRUS) is installed in each of the clusters. When the dRRUSis disposed in the private environments, it will be associatedwith multipath-rich and asynchronous delay propagation. Taking into account of this unique environment of private networks, asynchronous multiple signal reception is considered in the development of operation at the remote radio units to make an intersymbol interference free distributed cyclic delay diversity (dCDD) scheme for JT to achieve a full transmit diversity gain without full channel state information. A spectral efficiency of the proposed dCDD-based JT is analyzed by deriving the closedform expression, and then compared with link-level simulations for non-identically distributed frequency selective fading over the entire private network.

IEEE International Conference on Communications (ICC)

A Cluster-Based Transmit Diversity Scheme for Asynchronous Joint Transmissions in Private Networks

Kyeong Jin Kim, Jianlin Guo, Philip V. Orlik, Yukimasa Nagai, and H. Vincent Poor

***Abstract*—In this paper, a multiple cluster-based transmission diversity scheme is proposed for asynchronous joint transmissions (JT) in private networks, in which the use of multiple clusters or small cells is preferable to increase transmission speeds, reduce latency, and bring transmissions closer to the users. To increase the spectral efficiency and coverage, and to achieve flexible spatial degrees of freedom, a distributed remote radio unit system (dRRUS) is installed in each of the clusters. When the dRRUS is disposed in the private environments, it will be associated with multipath-rich and asynchronous delay propagation. Taking into account of this unique environment of private networks, asynchronous multiple signal reception is considered in the development of operation at the remote radio units to make an intersymbol interference free distributed cyclic delay diversity (dCDD) scheme for JT to achieve a full transmit diversity gain without full channel state information. A spectral efficiency of the proposed dCDD-based JT is analyzed by deriving the closed-form expression, and then compared with link-level simulations for non-identically distributed frequency selective fading over the entire private network.**

***Index Terms*—Private networks, distributed cyclic delay diversity, joint transmission, spectral efficiency.**

I. INTRODUCTION

A private network is a promising new connectivity model offering previously unavailable wireless network performance to businesses and individuals. The owners can optimize services at their specific areas by planning and installing their own networks, and ensure reliable communications by an exclusive use of available resources. Since they have complete control over every aspect of the network, they can determine how resources are utilized, how traffic is prioritized, how a specific security standard is deployed, and so on. Potential applications to industries, businesses, utilities, and public sectors have gravitated towards 5G wireless networks with increasingly stringent performance requirements, in terms of availability, reliability, latency, device density, and throughput [1]. The deployment of private networks can be feasible in the shared spectrum or unlicensed spectrum. Furthermore, to increase transmission speeds and capacity, reduce latency, and make the signal closer to the users, a dense deployment of small cells or clusters is expected [2].

To increase the spectral efficiency and coverage, a distributed antenna system (DAS) [3], [4], in which antennas are installed in a distributed manner over a coverage area of the base station (BS), is a promising approach for private networks. When each antenna operates as a BS, the DAS can be recognized as coordinated multiple point (CoMP) [5], [6]. Its core concept is to provide simultaneous communications by a plurality of BSs to a single or multiple users to improve the rate over a whole communication region. As major approaches of CoMP, coordinated beamforming and joint processing that includes joint transmissions (JT) are available. However, since we do not assume full channel state information at the transmitter (CSIT), we will focus on JT in this paper. Geographically placed BSs make the system properly counters path loss and shadowing [7]. However, it is challenging to collect full CSIT in the distributed system. Although a very reliable channel estimate can be obtained by the user, the feedback overhead will be overwhelming for large number of BSs. A conventional codebook based feeding back may not be working for CoMP due to significant differences in received signal strength [8].

In addition, a tight clock synchronization among BSs is required. Its mismatch will cause interference at the user due to the difference in signal arrival times from all the BSs. When Global Navigation Satellite System (GNSS) signals are not available in the private area, it is possible to achieve a desired clock synchronization by the precision time protocol (PTP) [9]. When a plurality of BSs transmit simultaneously, the existence of interference is an intrinsic problem [3] as well. We are investigating the following four problems in this paper.

1) When a DAS is installed in the private environments, it will be affected by multipath-rich propagation.
2) Since the distance between each of the remote radio units (RRUs) varies with respect to the receiver (RX), a received symbol timing cannot be aligned at the RX due to a path dependent propagation delay [10]. Note that RRU has only a single antenna and fixed power for simple processing, so that a system comprising a plurality of RRUs, called the distributed remote radio unit system (dRRUS), is recognized as the DAS [11].

K. J. Kim, J. Guo, and P. V. Orlik are with Mitsubishi Electric Research Laboratories (MERL), Cambridge, MA 02139 USA

Y. Nagai is with Mitsubishi Electric Corp., Japan

H. V. Poor is with the Department of Electrical Engineering, Princeton University, Princeton, NJ 08544 USA

This work was supported in part by the U.S. National Science Foundation under Grant CCF-1908308.

3) CSIT-dependent precoders are usually employed to minimize interference caused by simultaneous multiple transmissions. Thus, it is necessary to apply an interference-free transmission scheme to achieve a full transmit diversity.
4) Feeding back overhead from the RX increases in proportion to the number of RRUs.

Taking into four mentioned problems, we can summarize the following two key contributions comparing with existing work.

1) A new multi-cluster-based distributed remote radio unit system (MC-dRRUS): To provide a greater throughput for the private network, we propose a new MC-dRRUS, in which the private network server (PNS) provides transmission signals and synchronization to the respective cluster masters (CMs). Within non-overlapping clusters, each CM forms an individual dRRUS.
2) Distributed asynchronous cyclic delay diversity-based JT (dACDD-JT) scheme: It is desired to increase the number of RRUs to cover larger territory and to increase channel diversities. However, such an increase would result in additional interference, difficulty in time synchronization, and undesirable feedback overhead. With an available distribution for propagation delays over the whole paths, the CM is able to consider its variant in assigning the CDD delay at each of its RRUs, which is necessary to remove intersymbol interference (ISI) cased by asynchronous signal reception at the RX [12].

Notation: $\boldsymbol{I}_N$ denotes an $N \times N$ identity matrix; $\mathbf{0}$ denotes an all-zero matrix of with an appropriate size; and $\mathcal{CN}\left(\mu, \sigma^2\right)$ denotes a complex Gaussian distribution with mean μ and variance σ^2. The binomial coefficient is denoted by $\binom{n}{k} \triangleq \frac{n!}{(n-k)!k!}$. For a vector $\boldsymbol{a}$, $\mathbb{L}(\boldsymbol{a})$ denotes the cardinality; and its lth element is denoted by $\boldsymbol{a}(l)$. For another vector $\boldsymbol{a}_{i,N}$ with the second subscript defining its cardinality, $\mathrm{sum}(\boldsymbol{a}_{i,N}) = c$ denotes the sum for all set of positive indices of $\{\boldsymbol{a}_i(1), \ldots, \boldsymbol{a}_i(N)\}$ satisfying $\sum_{j=1}^{N} \boldsymbol{a}_i(j) = c$; and the binomial coefficient becomes the multinomial coefficient as follows: $\binom{c}{\boldsymbol{a}_{i,N}} \triangleq \frac{c!}{(\boldsymbol{a}_{i,N}(1))!(\boldsymbol{a}_{i,N}(2))!\ldots(\boldsymbol{a}_{i,N}(N))!}$. $\sum^{a}_{\substack{n_1,\ldots,n_J \\ n_1 \neq n_2 \neq \ldots \neq n_J}} \triangleq \sum^{a}_{n_1=1} \sum^{a}_{\substack{n_2=1 \\ n_2 \neq n_1}} \ldots \sum^{a}_{\substack{n_J=1 \\ n_J \neq n_1, \ldots, n_J \neq n_{J-1}}}$. For a set of continuous random variables, $\{x_1, x_2, \ldots, x_N\}$, $x_{\langle i \rangle}$ denotes the ith smallest random variable, so that it becomes the ith order statistic. For these order statistics, the spacing statistics, $\{y_1, \ldots, y_N\}$, are obtained by changing the variables as $y_i = x_{\langle i \rangle} - x_{\langle i-1 \rangle}$ with $y_1 = x_{\langle 1 \rangle}$.

II. System and Channel Models

Fig. 1 illustrates the considered MC-dRRUS with two non-overlapping and co-located clusters. Each cluster is recognized as an individual dRRUS. The PNS works as the grand master clock by PTP, so that it can compute propagation delay to the RX passing over a particular CM[1] and RRU. In contrast, the CM and RRUs work as the boundary clock and transparent

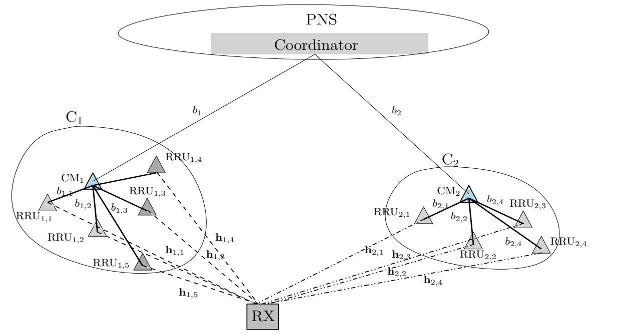

Fig. 1. Illustration of the proposed MC-dRRUS with five RRUs and four RRUs in each of the clusters. Two nodes highlighted in blue are assigned as CMs to control the RRUs within its cluster.

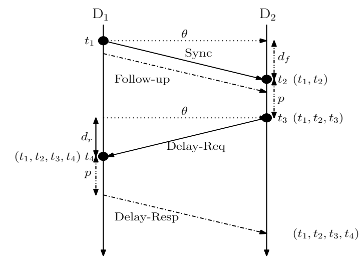

Fig. 2. Two-way packet exchange for synchronization. A filled circle dot denotes a timestamp in the event message recorded at its transmission and reception. The processing time taken at all the nodes is assumed to be p.

clocks, which have multiple PTP ports to interact with other clocks. The RX is represented as the ordinary clock. Very reliable main backhaul links, $\{b_1, b_2\}$, are configured to provide backhaul access to the clusters via the coordinator that resides at the PNS[2]. Other very reliable secondary backhaul links, $\{b_{i,j}, i = 1, 2, j = 1, \ldots, K\}$, provide backhaul access to RRUs via the CM. The CM controls all RRUs and is responsible for transmitting the signals. Every nodes in the cluster is assumed to be equipped with a single antenna.

A frequency selective fading channel from the kth RRU, deployed in the ith cluster, to the RX is denoted by $\boldsymbol{h}_{i,k}$ with $\mathbb{L}(\boldsymbol{h}_{i,k}) = N_{i,k}$. A distance-dependent large scaling fading is denoted by $\alpha_{i,k}$. For a distance $d_{i,k}$ from $\mathrm{RRU}_{i,k}$ to the RX, $\alpha_{i,k}$ is defined by $\alpha_{i,k} = (d_{i,k})^{-\epsilon}$, where ϵ denotes the path loss exponent. The RX is placed at a specific location with respect to the RRUs, and, thus, independent but non-identically distributed (i.n.i.d.) frequency selective fading channels from the RRUs to RX are assumed. The RX is assumed to have knowledge of the number of multipath components of the channels connected to itself by either sending a training sequence or adding a pilot as the suffix to each symbol block. To reduce the feedback overhead, the RX first computes $N_{\max} \triangleq \max\{N_{i,k}, \forall i, k\}$. After then, it feeds back $N_{\max}$ to the PNS, so that it is not necessary for the CMs to use X2 interface to exchange their channel relevant parameters.

To estimate the clock offset, θ, and propagation delay, d, PTP [9] specifies four event messages, such as Sync, Delay-Req, Pdelay-Req, and Pdelay-Resp, within which an accurate hardware timestamp is generated and recorded at transmission and reception of its respective messages. Thus,

[1]Access point can be work as the CM in IEEE 802.11be.

[2]Interested reader refer to [13] that investigates unreliable backhaul in the similar system setup. Thus, this paper does not consider unreliable backhaul.

after exchanging two-way packets between D_1 and D_2, four hardware timestamps, (t_1, t_2, t_3, t_4), are available at D_1 and D_2. Based on four timestamps, d and θ are respectively computed as: $d \approx \frac{(t_4+t_2)-(t_3+t_1)}{2}$ and $\theta \approx \frac{(t_3-t_1)-(t_4-t_2)}{2}$, where we assume that the forward propagation delay, d_f, is almost equal to the backward propagation delay, d_r, i.e., $d_f \approx d_r$, and clocks are perfectly synchronized in frequency and phase. Applying the same procedure, D_1 can estimate the propagation delay to another node, D_3, which supports PTP, so that it can be synchronized to D_2. This clock synchronization is accomplished via main and secondary backhaul links.

Referring to Figs. 1 and 2, the PNS has a set of propagation delay estimates $\{d_{1,k}\}_{k=1,\ldots,K}$ over the first cluster, C_1. For other clusters, the PNS can estimate propagation delay as well. Thus, we can assume that a complete set of propagation delays, $\{d_{i,k}\}_{i=1,\ldots,2,k=1,\ldots,K}$, is available at the PNS by employing PTP. According to this set, the PNS computes the propagation delay for the signal that arrives first at the RX as follows:

$$d_{\mathrm{ref}} \triangleq \min(\{d_{i,k}\}_{i=1,\ldots,2,k=1,\ldots,K}) \tag{1}$$

after then a relative propagation delay with respect to d_{ref},

$$\delta d_{i,k} \triangleq d_{i,k} - d_{\mathrm{ref}}, \text{for } i = 1, \ldots, 2, k = 1, \ldots, K. \tag{2}$$

The distributed CDD (dCDD) scheme was proposed by [11], [14] for distributed cyclic-prefixed single carrier (CP-SC) transmissions to achieve transmit diversity without full CSIT. Depending on the block size, Q, of the transmission symbol, $\boldsymbol{s} \in \mathbb{C}^{Q\times 1}$, and the cyclic-prefix (CP) length, N_{CP}, which is set to $N_{\max}$, the maximum number of RRUs that achieves ISI-free reception at the RX is determined by $M = \lfloor Q/N_{\mathrm{CP}} \rfloor$, where $\lfloor \cdot \rfloor$ denotes the floor function. When the ith dRRUS is overpopulated with the RRUs, i.e., $K_i > M$, the CM_i needs to select only M RRUs for dCDD operation. Thus, the RX needs to feed back necessary information to the PNS. Based on available channel estimates, the RX rearranges them according to their strength, from smallest to largest, as follows:

$$\alpha_{i,\langle 1\rangle} \|\boldsymbol{h}_{i,\langle 1\rangle}\|^2 \leq \ldots \leq \alpha_{i,\langle K_i\rangle} \|\boldsymbol{h}_{i,\langle K_i\rangle}\|^2. \tag{3}$$

According to (3), the RX forms a list specifying the strength order, that is, $\mathbb{D}_i \triangleq (\langle 1\rangle, \ldots, \langle M\rangle)$, and then feeds back $\mathbb{D}_i$ to the PNS. Furthermore, CM_i can have $\mathbb{D}_i$ via the main backhaul communications over b_i, from which CM_i selects M RRUs indexed by the last M elements of $\mathbb{D}_i$, that is, $\mathrm{RRU}_{i,\langle K-M+1\rangle}, \ldots, \mathrm{RRU}_{i,\langle K\rangle}$. The remaining $K-M$ RRUs are controlled by CM_i to be idle from communications. For the chosen M RRUs, CM_i assigns the CDD delay to $\mathrm{RRU}_{i,\langle K-M+m\rangle}$ as follows:

$$\Delta_m = (m-1)N_{\mathrm{CP}},\ m = 1, \ldots, M. \tag{4}$$

Thus, for an overpopulated dRRUS, the PNS can achieve the same objective as distributed MRT (dMRT) with using only partial CSIT. In summary, for dCDD operation, CM_i needs to know M, N_{CP}, and $\mathbb{D}_i$, which are available at each of the CMs by backhaul communications made by the PNS.

III. dACDD-JT for CP-SC Transmissions

Without loss of generality, we assume that $\mathrm{RRU}_{1,1}$'s signal arrives first at the RX in the considered private networks. Since the PNS has propagation delay estimates for its whole network, it can compute the distribution for relative propagation delays with respect to $\mathrm{RRU}_{1,1}$'s signal. As an initial interactive process between the PNS and RX, the PNS transmits d_{ref} to the RX via clusters.

After the removal of the CP signal and applying post-processing by $d_{1,1}$, the RX receives a composite signal from two clusters as follows:

$$\boldsymbol{r} = \sum_{m=1}^{M} \Big[\big[\boldsymbol{\Pi}_{1,\langle K-M+m\rangle} \boldsymbol{H}_{1,\langle K-M+m\rangle} \boldsymbol{P}_{1,\langle K-M+m\rangle} \boldsymbol{s}\big]_{J_1} + \big[\boldsymbol{\Pi}_{2,\langle K-M+m\rangle} \boldsymbol{H}_{2,\langle K-M+m\rangle} \boldsymbol{P}_{2,\langle K-M+m\rangle} \boldsymbol{s}\big]_{J_2} \Big] + \boldsymbol{z} \tag{5}$$

where $[\cdot]_{J_1}$ and $[\cdot]_{J_2}$ respectively represent signals transmitted from C_1 and C_2. In addition, $\boldsymbol{H}_{i,\langle K-M+m\rangle}$ is right circulant matrix determined by $\sqrt{P_T \alpha_{i,\langle K-M+m\rangle}} \boldsymbol{h}_{i,\langle K-M+m\rangle}$ with P_T denoting the transmission power for single carrier transmissions. Note that $\boldsymbol{\Pi}_{i,\langle K-M+m\rangle}$ is right circulant and orthogonal permutation matrix determined by a relative propagation delay, $\delta d_{i,\langle K-M+m\rangle}$. Since full CSIT is not available in the considered system, the same P_T is assigned to all the RRUs. By shifting down $\boldsymbol{I}_Q$ by $\delta d_{i,\langle K-M+m\rangle}$ rows, $\boldsymbol{\Pi}_{i,\langle K-M+m\rangle}$ can be obtained. An additional set of permutation matrices, $\{\boldsymbol{P}_{i,\langle K-M+m\rangle}, \forall i, m\}$, will be defined later. The additive vector noise is denoted by $\boldsymbol{z} \sim \mathcal{CN}(\boldsymbol{0}, \sigma_z^2 \boldsymbol{I}_Q)$. For proper operation, we assume that $0 \leq d_{i,\langle K-M+m\rangle} \leq N_{\mathrm{CP}}$, so that we have $0 \leq \delta d_{i,\langle K-M+m\rangle} \leq N_{\mathrm{CP}}$ [10].

A. dACDD for JT

Using the properties of the right circulant matrix, (5) can be rewritten as:

$$\boldsymbol{r} = \sum\nolimits_{m=1}^{M} \Big[\boldsymbol{H}_{1,\hat{m}} \boldsymbol{\Pi}_{1,\hat{m}} [\boldsymbol{P}_{1,\hat{m}} \boldsymbol{s}]_{J_3} + \boldsymbol{H}_{2,\hat{m}} \boldsymbol{\Pi}_{2,\hat{m}} [\boldsymbol{P}_{2,\hat{m}} \boldsymbol{s}]_{J_4} \Big] + \boldsymbol{z} \tag{6}$$

where $\hat{m} \triangleq \langle K-M+m\rangle$. Furthermore, $[\cdot]_{J_3}$ and $[\cdot]_{J_4}$ correspond to local operations respectively performed at $\mathrm{RRU}_{1,\hat{m}}$ and $\mathrm{RRU}_{2,\hat{m}}$. To make ISI-free reception at the RX, it is required that $\boldsymbol{\Pi}_{1,\hat{m}} \boldsymbol{P}_{1,\hat{m}}$ and $\boldsymbol{\Pi}_{2,\hat{m}} \boldsymbol{P}_{2,\hat{m}}$ are orthogonal and right circulant matrices, and meet the CDD delay assignment for $\mathrm{RRU}_{i,\hat{m}}$. Accordingly, we can readily obtain $\delta T_{i,\hat{m}}$ that meets the condition: $\Delta_{\hat{m}} = \delta d_{i,\hat{m}} + \delta T_{i,\hat{m}}$. For operation $[\cdot]_{J_3}$, $\mathrm{RRU}_{1,\hat{m}}$ assigns $\delta T_{1,\hat{m}}$ as its CDD delay rather than $\Delta_{\hat{m}}$. By circularly shifting down the transmission symbol $\boldsymbol{s}$ by $\delta T_{1,\hat{m}}$, operation $[\cdot]_{J_3}$ can be accomplished. Similar operation is conducted for $[\cdot]_{J_4}$. Thus, $\boldsymbol{P}_{1,\hat{m}}$ and $\boldsymbol{P}_{2,\hat{m}}$ can be obtained from $\boldsymbol{I}_Q$ by circularly shifting down respectively by $\delta T_{1,\hat{m}}$ and $\delta T_{2,\hat{m}}$.

ISI caused by a variant propagation delay and multiple transmissions can be removed by a series of circular shifting operations that are respectively performed by the RRUs, and caused by propagation. Thus, dACDD is an extensive version of dCDD allowing the distribution of propagation delays over the private network. For proper dACDD operation, the PNS is required to know $\{d_{i,\hat{m}}\}_{i=1,2;m=1,\ldots,M}$ and $\{\delta d_{i,\hat{m}}\}_{i=1,2;m=1,\ldots,M}$. However, due to the use of PTP, an additional feedback is not necessary from the RX, which is the key difference from [12].

IV. Spectral Efficiency of JT by Asynchronous MC-dACDD

Using the properties of the right circulant matrix, the achievable signal-to-noise ratio (SNR) realized by MC-dACDD based JT can be derived by the following *Theorem 1*.

Theorem 1: Even for asynchronous signal reception at the RX, ISI-free reception can be achieved via MC-dACDD. Thus, the achievable SNR realized by JT is given by

$$\gamma_{\mathrm{JT}} = \gamma_{\mathrm{JT},1} + \gamma_{\mathrm{JT},2} = \rho_s/\sigma_z^2 \tag{7}$$

where $\rho_s = P_T\big(\sum_{m=1}^{M} \alpha_{1,\hat{m}}\|\boldsymbol{h}_{1,\hat{m}}\|^2 + \sum_{m=1}^{M} \alpha_{2,\hat{m}}\|\boldsymbol{h}_{2,\hat{m}}\|^2\big)$ with $\rho \stackrel{\triangle}{=} P_T/\sigma_z^2$ and $\gamma_{\mathrm{JT},i} \stackrel{\triangle}{=} \rho\sum_{m=1}^{M}\alpha_{i,\hat{m}}\|\boldsymbol{h}_{i,\hat{m}}\|^2$.

Proof: When $\{\boldsymbol{h}_{1,\hat{m}}, \forall m\}$ and $\{\boldsymbol{h}_{2,\hat{m}}, \forall m\}$ are independent of each other, ρ_s, realized at the RX, is determined by the summation of their squared Euclidean norms. ■

For overpopulated dRRUS, the CM selects only M RRUs by referring to the channel strength. Thus, the order statistics are employed in the expression for the achievable SNR. *Theorem 1* proves that by compensating different signal arrival times at the RX, the MC-dACDD makes JT provide the same benefit as dMRT without full CSIT at the PNS and CMs.

Theorem 2: Due to the use of JT, the proposed MC-dACDD results in the SNR, γ_{JT} realized at the RX, whose approximation of the moment generating function (MGF) is given by

$$M_{\gamma_{\mathrm{JT}}}(s) = \widetilde{\sum_{\substack{n_1,\ldots,n_M\\ n_1\neq\ldots\neq n_M}}} \widehat{\sum_{\substack{\tilde{n}_1,\ldots,\tilde{n}_M\\ \tilde{n}_1\neq\ldots\neq\tilde{n}_M}}} \prod_{k=1}^{M}(M+1-k)^{-e_k}\Gamma(e_k) \prod_{k=1}^{M}\Big((M+1-k)^{-\tilde{e}_k}\Gamma(\tilde{e}_k)\Big)\sum_{l=0}^{N_1}\big(\delta_l(b_I)^{-l} (1/b_I+s)^{-G_d-l}\big) \tag{8}$$

where $G_d \stackrel{\triangle}{=} \sum_{k=1}^{2M} E_k$, $b_I \stackrel{\triangle}{=} \min(1/Q_1,\ldots,1/Q_{2M})$ with Q_k and E_k, respectively the kth elements of $\boldsymbol{Q} = [q_1,\ldots,q_M,\tilde{q}_1,\ldots,\tilde{q}_M]^T$ and $\boldsymbol{E} = [e_1,\ldots,e_M,\tilde{e}_1,\ldots,\tilde{e}_M]^T$. Furthermore, N_1 denotes an upper limit summation, and $\delta_l \stackrel{\triangle}{=} \frac{1}{l}\sum_{i=1}^{l} i r_i \delta_{l-i}$ with $\delta_0 = 1$ and $r_i = \sum_{j=1}^{2M} E_j(1-b_I Q_i)^j$. Additional terms specified in (8) are defined in Appendix A.

Proof: See Appendix A. ■

Theorem 2 provides the MGF expressed by the weighted sum of N_1+1 terms, proportional to $(1/b_I+s)^{-G_d-l}$.

Corollary 1: The CDF of γ_{JT} can be expressed by a finite number of gamma distributions.

$$F_{\gamma_{\mathrm{JT}}}(x) = 1 - \widetilde{\sum_{\substack{n_1,\ldots,n_M\\ n_1\neq\ldots\neq n_M}}} \widehat{\sum_{\substack{\tilde{n}_1,\ldots,\tilde{n}_M\\ \tilde{n}_1\neq\ldots\neq\tilde{n}_M}}} \prod_{k=1}^{M}(M+1-k)^{-e_k} \Gamma(e_k)\prod_{k=1}^{M}(M+1-k)^{-\tilde{e}_k}\Gamma(\tilde{e}_k)\sum_{l=0}^{N_1}\delta_l(b_I)^{-l} ((b_I)^{G_d+l}/\Gamma(G_d+l))\Gamma_U(G_d+l, x/b_I) \tag{9}$$

where $\Gamma(\cdot)$ and $\Gamma_U(\cdot,\cdot)$ respectively denote complete gamma and incomplete upper-gamma functions.

Based on (9), the spectral efficiency (SE) of the proposed MC-dACDD is given by the following theorem.

Theorem 3: The achievable SE of the proposed MC-dACDD is given by

$$\mathrm{SE} = \frac{1}{\log(2)} \widetilde{\sum_{\substack{n_1,\ldots,n_M\\ n_1\neq\ldots\neq n_M}}} \widehat{\sum_{\substack{\tilde{n}_1,\ldots,\tilde{n}_M\\ \tilde{n}_1\neq\ldots\neq\tilde{n}_M}}} \prod_{k=1}^{M}(M+1-k)^{-e_k} \Gamma(e_k)\prod_{k=1}^{M}(M+1-k)^{-\tilde{e}_k}\Gamma(\tilde{e}_k)(b_I)^{G_d} \Big[\sum_{l=0}^{N_1}\frac{\delta_l}{\Gamma(G_d+l)}G_{2,3}^{3,1}\Big(1/b_I\Big|\begin{smallmatrix}0,1\\ G_d+l,0,0\end{smallmatrix}\Big)\Big] \tag{10}$$

where $G_{p,q}^{m,n}\Big(t\Big|\begin{smallmatrix}a_1,\ldots,a_n,a_{n+1},\ldots,a_p\\ b_1,\ldots,b_m,b_{m+1},\ldots,b_q\end{smallmatrix}\Big)$ denotes the Meijer G-function [15, Eq. (9.301)].

Proof: We first express the functions of x in terms of Meijer G-functions, i.e., $(1+x)^{-1} = G_{1,1}^{1,1}\Big(x\Big|\begin{smallmatrix}0\\ 0\end{smallmatrix}\Big)$ and $\Gamma_u(j,\alpha x) = G_{1,2}^{2,0}\Big(\alpha x\Big|\begin{smallmatrix}1\\ j,0\end{smallmatrix}\Big)$. After this, applying [16, eq. (2.24.1,2)], we can derive (10). ■

V. Simulation results

We assume the following simulation setup.

1) C_1: Six RRUs are placed at $(-1.2, 4.7)$, $(0.7, 4.0)$, $(3.0, 3.0)$, $(-2.5, 2.7)$, $(-3.3, 0.4)$, and $(-3.0, 3.5)$. The first cluster master, CM_1, is placed at $(0, 2)$ in a 2-D plane.
2) C_2: Four RRUs are placed at $(12.8, 3.3)$, $(7.4, 2.5)$, $(10.0, 4.6)$, and $(9.0, 1.7)$. The second cluster master, CM_2, is placed at $(10.0, 3.0)$ in a 2-D plane.
3) For CP-SC transmissions, we assume that $Q = 32$ and $N_{\mathrm{CP}} = 8$. Thus, the CMs can support up to four RRUs for dACDD operation, i.e., $M = 4$.
4) RX is placed at $(3, -3)$.
5) In all scenarios, we fix $P_T = 1$. A fixed path-loss exponent is assumed to be $\epsilon = 2.09$.
6) The relative time difference, $\delta T_{i,m}$, between the arrival time of the signal transmitted from $\mathrm{RRU}_{i,m}$ with respect to $\mathrm{RRU}_{i,1}$ is represented as an integer value uniformly generated between 0 and N_{CP}.

We consider several frequency selective fading channel parameters for two clusters depending on the respective number of RRUs, K_1 and K_2. For notation purpose, we use $\mathcal{H}_1 = \{N_{1,j}, j = 1,\ldots,K_1\}$ for C_1 and $\mathcal{H}_2 = \{N_{2,j}, j = 1,\ldots,K_2\}$ for C_2.

1) $\mathcal{X}_1$: $\mathcal{H}_1 = \{2,3,4,2,3\}$ and $\mathcal{H}_2 = \{3,2,3,3\}$.
2) $\mathcal{X}_2$: $\mathcal{H}_1 = \{3,4,2,3,2\}$ and $\mathcal{H}_2 = \{3,2,3,3\}$.
3) $\mathcal{X}_3$: $\mathcal{H}_1 = \{2,3,4,2,3,4\}$ and $\mathcal{H}_2 = \{3,2,3,3,4\}$.
4) $\mathcal{X}_4$: $\mathcal{H}_1 = \{2,3,4\}$ and $\mathcal{H}_2 = \{3,2,3\}$.
5) $\mathcal{X}_5$: $\mathcal{H}_1 = \{3,4,5,3,4,5\}$ and $\mathcal{H}_2 = \{5,4,5,5,5\}$.

We denote the analytically derived SE by **An**, whereas we denote the exact performance metric obtained by the link-level simulations by **Ex** in the sequel. Since there is no existing similar setup, i.e., CP-SC based MC-dACDD with JT, we mainly focus on the proposed scheme in this paper.

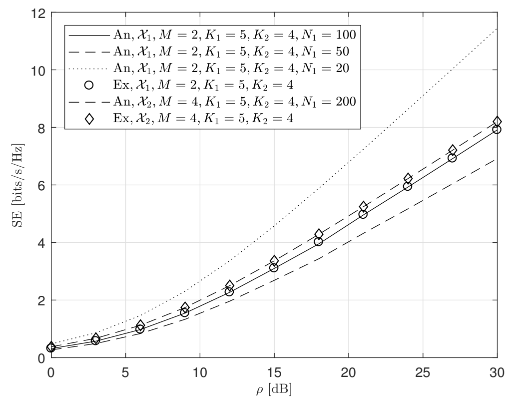

Fig. 3. SE for various system and channel parameters.

We first verify the analytically derived SEs for two overpopulated systems. The first system with $\mathcal{X}_1$ assumes that dACDD supports only two RRUs, while five and four RRUs exist in C_1 and C_2, respectively. For the second system with $\mathcal{X}_2$, dACDD supports only four RRUs, while five and four RRUs exist in C_1 and C_2, respectively. Fig. 3 shows an accuracy of the analytically derived SEs comparing with the exact SEs. This figure also shows that if N_1 is not sufficiently large, an approximation, which is used in *Theorem 2*, does not provide an accurate SE. Thus, in the sequel, we use a sufficiently large value for N_1 without a specific description for it. In general, as M increases, a larger value for N_1 is required to obtain very reliable and accurate analytic SEs.

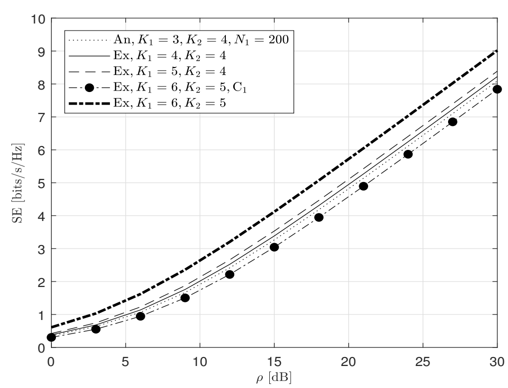

Fig. 4. SE for various over-popularity of dRRUSs with $\mathcal{X}_3$.

In generating Fig. 4, we mainly use $\mathcal{X}_3$ with various over-popularity of dRRUSs and assume that $M=4$. From Fig. 4 we can extract the following facts:

- As the dRRUS is populated with more RRUs, a greater SE can be achieved.
- As the number of clusters increases, a greater SE can be achieved. However, a more tight restriction on the number of RRUs for dCDD exists due to different frequency selective fading severity across deployed clusters.

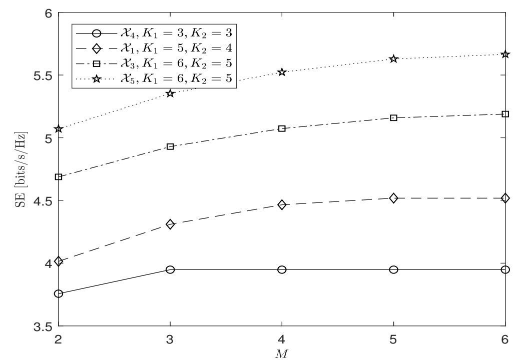

Fig. 5. SE for various values of M and different numbers of multipath components.

At a fixed 18 dB SNR, Fig. 5 shows the SE for various system and channel parameters. For underpopulated and overpopulated dRRUSs, the impact of M on the SE is investigated.

- For a given K_1 and K_2, as M increases, the dRRUS is populated with less RRUs. Although the SE increases in proportion to M, the growth rate of the SE decreases.
- As K_1 or K_2 greater, the growth rate of the SE increases. For example, $(K_1=6, K_2=5)$ vs. $(K_1=5, K_2=4)$.
- As the number of multipath components increases, a greater SE is obtained. For example, $\mathcal{X}_3$ vs. $\mathcal{X}_5$.

VI. Conclusions

In this paper, we have proposed a multiple cluster-based transmit diversity scheme for asynchronous joint transmissions. To relax the requirement of full channel state information at the private network server and deal with different propagation over the paths of the distributed systems composed of remote radio units, a dACDD scheme has been developed to the private network. The multi-level hierarchical PTP allows to break the dependency of different dRRUS clusters from a common PNS allowing each dRRUS cluster to use dACDD independently from other clusters. For i.n.i.d. frequency selective fading channels, a new closed-form expression for the spectral efficiency has been derived. Its accuracy has been also verified comparing with the link-level simulations. By integrating a transmission scheme, propagation delay estimation, and operation at the RRUs effectively, we have seen that the proposed multiple cluster-based asynchronous joint transmissions can achieve the desired spectral efficiency for various simulations scenarios.

Appendix A: Proof of Theorem 2

To simplify the notation, let us define x_m as $x_m \triangleq \rho\alpha_{1,\langle K_1-M+m\rangle}\|\boldsymbol{h}_{1,\langle K_1-M+m\rangle}\|^2$. Note that the order statistics are implicitly involved in this definition. We mainly focus on the derivation of the distribution for $\gamma_{\mathrm{JT},1}$ in the sequel. The MGF of $\gamma_{\mathrm{JT},1}$ can be defined as

$$M_{\gamma_{\mathrm{JT},1}}(s)=\sum^{K_1}_{\substack{n_1,\ldots,n_M\\ n_1\neq n_2\neq\ldots\neq n_M}}\int_0^\infty\int_{x_1}^\infty\cdots\int_{x_{M-2}}^\infty\int_{x_{M-1}}^\infty \Big[\prod_{i=1}^M\left((b_i)^{p_i}/\Gamma(p_i)\right)(x_i)^{p_i-1}e^{-(s+b_i)x_i}\prod_{i=M+1}^{K_1}\gamma_l(p_i,b_ix_1)/\Gamma(p_i)\Big]_{J6}\, dx_M\ldots dx_2dx_1$$

where $\gamma_l(\cdot,\cdot)$ denotes the incomplete lower-gamma function, $p_i\triangleq N_{1,\langle K_1-M+n_i\rangle}$, and $b_i\triangleq\frac{1}{\rho\alpha_{1,\langle K_1-M+n_i\rangle}}$. Next, we rewrite $\gamma(p_i,b_ix_1)/\Gamma(p_i)$ as follows:

$$\frac{\gamma(p_i,b_ix_1)}{\Gamma(p_i)}=\sum_{\mathrm{sum}(\boldsymbol{a}_{i,p_i+1})=1}\binom{1}{\boldsymbol{a}_{i,p_i+1}}X_i x_1^{\tilde{p}_i}e^{-\lambda_ib_ix_1}\quad(\mathrm{A.1})$$

where $\lambda_i\triangleq\sum_{j=2}^{p_i+1}\boldsymbol{a}_i(j)$, $\theta_i\triangleq\prod_{j=2}^{p_i}(\Gamma(j))^{\boldsymbol{a}_i(j+1)}$, $\tilde{p}_i\triangleq\sum_{j=3}^{p_i+1}(j-2)\boldsymbol{a}_i(j)$, and $X_i\triangleq(-1)^{\lambda_i}(b_i)^{\tilde{p}_i}/\theta_i$ for $\boldsymbol{a}_i$s. Thus, we can evaluate $[\cdot]_{J_6}$ as follows:

$$[\cdot]_{J_6}=\sum_{\substack{n_1,\ldots,n_M\\ n_1\neq n_2\neq\ldots\neq n_M}}\prod_{i=1}^M\frac{(b_i)^{p_i}}{\Gamma(p_i)}\sum_{\mathrm{sum}(\boldsymbol{a}_{M+1,p_{M+1}+1})=1}\cdots\sum_{\mathrm{sum}(\boldsymbol{a}_{K_1,p_{K_1}+1})=1}\binom{1}{\boldsymbol{a}_{M+1,p_{M+1}+1}}\cdots\binom{1}{\boldsymbol{a}_{K_1,p_{K_1}+1}}\Big(\prod_{i=M+1}^{K_1}X_i\Big)\Big[(x_1)^{p_1+\tilde{p}_{M+1}+\ldots+\tilde{p}_{K_1}-1} e^{-(s+b_1+\lambda_{M+1}b_{M+1}+\ldots+\lambda_{K_1}b_{K_1})y_1}(x_2)^{p_2-1}e^{-(s+b_2)x_2}\ldots (x_M)^{p_M-1}e^{-(s+b_M)x_M}\Big]_{J_7}.\quad(\mathrm{A.2})$$

Now replacing x_i with $x_i=\sum_{j=1}^i y_j$, where $\{y_1,\ldots,y_N\}$ are the spacing statistics of the order statistics, $\{x_1,\ldots,x_M\}$, $[\cdot]_{J_7}$ can be expressed as follows:

$$[\cdot]_{J_7}=\sum_{\mathrm{sum}(\boldsymbol{a}_{2,p_2})=p_2-1}\cdots\sum_{\mathrm{sum}(\boldsymbol{a}_{M,p_M})=p_M-1}\binom{p_2-1}{\boldsymbol{a}_{2,p_2}}\cdots\binom{p_M-1}{\boldsymbol{a}_{M,p_M}}(y_1)^{p_1+\sum_{j=2}^M a_{j,1}+\tilde{p}_{M+1}+\ldots+\tilde{p}_{K_1}-1} e^{-(Ms+\sum_{j=1}^M b_j+\sum_{j=M+1}^{K_1}\lambda_jb_j)y_1}(y_2)^{\sum_{j=2}^M a_{j,2}} e^{-((M-1)s+\sum_{j=2}^{K_1}b_j)y_2}\ldots(y_M)^{a_{M,M}}e^{-(s+b_M)y_M}\quad(\mathrm{A.3})$$

where we use the multinomial and binomial theorems in the derivation. Now using the spacing statistics, $\{y_i\}$ becomes independent, so that (A.1) is given by

$$M_{\gamma_{\mathrm{JT},1}}(s)=\widetilde{\sum}_{\substack{n_1,\ldots,n_M\\ n_1\neq n_2\neq\ldots\neq n_M}}\prod_{k=1}^M(M+1-k)^{-e_k}\Gamma(e_k)\prod_{k=1}^M(s+q_k)^{-e_k}$$

where

$$\widetilde{\sum}_{\substack{n_1,\ldots,n_M\\ n_1\neq n_2\neq\ldots\neq n_M}}\triangleq\sum^{K_1}_{\substack{n_1,\ldots,n_M\\ n_1\neq n_2\neq\ldots\neq n_M}}A_{M_1}\sum_{\mathrm{sum}(\boldsymbol{a}_{M+1,p_{M+1}+1})=1}\cdots\sum_{\mathrm{sum}(\boldsymbol{a}_{K_1,p_{K_1}+1})=1}\Big[\prod_{j=M+1}^{K_1}\binom{1}{\boldsymbol{a}_{j,p_j+1}}\Big]\Big[\prod_{i=M+1}^{K_1}X_i\Big]\sum_{\mathrm{sum}(\boldsymbol{a}_{2,p_2})=p_2-1}\cdots\sum_{\mathrm{sum}(\boldsymbol{a}_{M,p_M})=p_M-1}\Big[\prod_{j=2}^M\binom{p_j-1}{\boldsymbol{a}_{j,p_j}}\Big],$$

$e_1\triangleq p_1+\sum_{j=2}^M\boldsymbol{a}_j(1)+\sum_{j=M+1}^{K_1}\tilde{p}_j$, $e_{k\geq2}\triangleq\sum_{j=2}^M\boldsymbol{a}_j(k)+1$, $q_1\triangleq\frac{1}{M}\big(\sum_{j=1}^Mb_j+\sum_{j=M+1}^{K_1}\lambda_jb_j\big)$, and $q_{k\geq2}\triangleq\frac{1}{M+1-k}\big(\sum_{j=k}^Mb_j\big)$.

With an assumption that M RRUs, out of K_2 RRUs, are selected by CM_2, the MGF of $\gamma_{\mathrm{JT},2}$ can be derived as $\gamma_{\mathrm{JT},1}$ with $\widehat{\sum}_{\substack{n_1,\ldots,n_M\\ n_1\neq n_2\neq\ldots\neq n_M}}$ similarly defined as $\widetilde{\sum}_{\substack{n_1,\ldots,n_M\\ n_1\neq n_2\neq\ldots\neq n_M}}$ and with $\hat{p}_i\triangleq N_{2,\langle K_2-M+\hat{n}_i\rangle}$, $\hat{b}_i\triangleq\frac{1}{\rho\alpha_{2,\langle K_2-M+\hat{n}_i\rangle}}$, $\hat{A}_M\triangleq\prod_{i=1}^M\frac{(\hat{b}_i)^{\hat{p}_i}}{\Gamma(\hat{p}_i)}$, $\hat{\lambda}_i\triangleq\sum_{j=2}^{\hat{p}_i+1}\hat{\boldsymbol{a}}_i(j)$, $\hat{\theta}_i\triangleq\prod_{j=2}^{\hat{p}_i}(\Gamma(j))^{\hat{\boldsymbol{a}}_i(j+1)}$, $\tilde{\hat{p}}_i\triangleq\sum_{j=3}^{\hat{p}_i+1}(j-2)\hat{\boldsymbol{a}}_i(j)$, and $\hat{X}_i\triangleq\frac{(-1)^{\hat{\lambda}_i}(\hat{b}_i)^{\tilde{\hat{p}}_i}}{\hat{\theta}_i}$ for $\hat{\boldsymbol{a}}_i$s. $\tilde{e}_k$ and $\tilde{q}_k$ are defined as those of e_k and q_k. Since the SNR realized at the RX is the sum of two RVs, $\gamma_{\mathrm{JT},1}$ and $\gamma_{\mathrm{JT},2}$, the MGF is given by

$$M_{\gamma_{\mathrm{JT}}}(s)=\widetilde{\sum}_{\substack{n_1,\ldots,n_M\\ n_1\neq\ldots\neq n_M}}\widehat{\sum}_{\substack{\tilde{n}_1,\ldots,\tilde{n}_M\\ \tilde{n}_1\neq\ldots\neq\tilde{n}_M}}\prod_{k=1}^M(M+1-k)^{-e_k}\Gamma(e_k)\prod_{k=1}^M(M+1-k)^{-\tilde{e}_k}\Gamma(\tilde{e}_k)\prod_{k=1}^M(s+q_k)^{-e_k}\prod_{k=1}^M(s+\tilde{q}_k)^{-\tilde{e}_k}.\quad(\mathrm{A.4})$$

Now applying the approach proposed by [17], we can derive (8).

References

[1] J. Mietzner, "A survey of resource management toward 5G radio access networks," *IEEE Commun. Surveys Tuts.*, vol. 18, no. 3, pp. 1656–1686, 2016.

[2] H. Li, J. Hajipour, A. Attar, and V. C. M. Leung, "Efficient HetNet implementation using broadband wireless access with fiber-connected massively distributed antennas architecture," *IEEE Wireless Commun.*, vol. 18, no. 3, pp. 72–78, Jun. 2011.

[3] X. Zhang *et al.*, "Distributed power allocation for coordinated multipoint transmissions in distributed antenna systems," *IEEE Trans. Wireless Commun.*, vol. 12, no. 5, pp. 2281–2291, May 2013.

[4] W. Feng *et al.*, "Virtual MIMO in multi-cell distributed antenna systems: Coordinated transmissions with large-scale CSIT," *IEEE J. Sel. Areas Commun.*, vol. 31, no. 10, pp. 2067–2081, Oct. 2013.

[5] X. Tao, X. Xu, and Q. Cui, "An overview of cooperative communications," *IEEE Commun. Mag.*, pp. 65–71, Jun. 2012.

[6] V. Garcia, Y. Zhou, and J. Shi, "Coordinated multipoint transmission in dense cellular networks with user-centric adaptive clustering," *IEEE Trans. Wireless Commun.*, vol. 13, no. 8, pp. 4297–4308, Aug. 2014.

[7] H. Zhuang, L. Dai, L. Xiao, and Y. Yao, "Spectral efficiency of distributed antenna system with random antenna layout," *Electronics Letters*, vol. 39, no. 6, pp. 495–496, Mar. 2003.

[8] R. Heath, S. Peters, Y. Wang, and J. Zhang, "A current perspective on distributed antenna systems for the downlink of cellular systems," *IEEE Commun. Mag.*, pp. 161–167, Apr. 2013.

[9] A. Mahmood, R. Exel, H. Trsek, and T. Sauter, "Clock synchronization over IEEE 802.11–A survey of methodologies and protocols," *IEEE Trans. Ind. Informat.*, vol. 13, no. 2, pp. 907–922, Apr. 2017.

[10] H. Wang, "Full-diversity uncoordinated cooperative transmission for asynchronous relay networks," *IEEE Trans. Veh. Technol.*, vol. 66, no. 1, pp. 1939–9359, Jan. 2017.

[11] K. J. Kim, M. D. Renzo, H. Liu, P. V. Orlik, and H. V. Poor, "Performance analysis of distributed single carrier systems with distributed cyclic delay diversity," *IEEE Trans. Commun.*, vol. 65, no. 12, pp. 5514–5528, Dec. 2017.

[12] K. J. Kim, H. Liu, M. Wen, P. V. Orlik, and H. V. Poor, "Secrecy performance analysis of distributed asynchronous cyclic delay diversity-based cooperative single carrier system," *IEEE Trans. Commun.*, vol. 68, no. 5, pp. 2680–2694, May 2020.

[13] K. J. Kim, H. Liu, P. L. Yeoh, P. V. Orlik, and H. V. Poor, "Backhaul reliability analysis on cluster-based transmit diversity schemes in private networks," in *Proc. IEEE Global Commun. Conf.*, Taipei, Taiwan, Dec. 2020, pp. 1–6.

[14] K. J. Kim, H. Liu, Z. Ding, P. V. Orlik, and H. V. Poor, "Diversity gain analysis of distributed CDD systems in non-identical fading channels," *IEEE Trans. Commun.*, vol. 68, no. 11, pp. 7218–7231, Nov. 2020.

[15] I. S. Gradshteyn and I. M. Ryzhik, *Table of Integrals, Series, and Products*. New York: Academic Press, 2007.

[16] A. P. Prudnikov, Y. A. Brychkov, and O. I. Marichev, *Integral and Series. Vol. 3: More Special Functions*, 3rd ed. London: Gordon and Breach, 1992.

[17] P. G. Moschopoulos, "The distribution of the sum of independent gamma random variables," *Ann. Inst. Statist. Math. (PartA)*, vol. 37, pp. 541–544, 1985.